Adaptive Torque Control of Permanent Magnet Synchronous Motors in Automotive Applications

Jérémy Malaizé[(1)], Wissam Dib[(2)] and Sylvain Toru.
[(1)] jeremy.malaize@ifp.fr [(2)] wissam.dib@ifp.fr
[(1,2)] IFP, 1 et 4 avenue de Bois-Préau
92852 Rueil-Malmaison Cedex, France

***Abstract*— In this paper, an adaptive torque control scheme for Permanent Magnet Synchronous Motors (PMSM) used in automotive applications is presented. The proposed algorithm relies on stator currents and rotor speed measurements and achieves global asymptotic convergence of the torque to its desired time-varying reference. The appealing feature of the proposed scheme is that little information about the motor to control is required, since the main physical parameters are estimated online. In order to make the scheme robust to stator resistance and magnetic flux variations due to temperature changes, a nonlinear estimator is designed to asymptotically estimate the unknown parameters. Moreover, a novel approach to estimate the saliency parameters and the position at standstill is also proposed. The relevancy of the proposed strategy is verified via both simulation and experimental results.**

I. Introduction

Permanent magnet synchronous motors (PMSMs) are widely used in high performance variable frequency drives, especially for electric or hybrid operated vehicles [13]. Their popularity is justified by several advantages over commonly used motors. The absence of the external rotor excitation eliminates rotor losses and makes PMSMs highly efficient. In addition, the absence of rotor windings renders brushes obsolete, and thus reduces the maintenance costs [12], [17].

Classical research on control of PMSM has focused on stability of the rotor position and velocity. Several stable position and velocity controllers have been reported in the control and industrial literature [15], [16].

In this paper, our concern is to control the torque of produced by PMSM, which is essential in hybrid and electrical vehicles applications. The control objective considered hereafter is to respond to a torque request in a precise, fast and repeatable way, whether for a full electric vehicle, or an hybrid electric vehicle. In the first case, the driver is directly responsible for this request and, for driveability reasons, the torque response is not expected to drift in time along the considered travel. In the latter case, the torque demand is computed by an electronic control unit in charge of splitting the driver torque request downstream to a PMSM and an internal combustion engine [3], [18]. The main concern here is to optimize the vehicle fuel consumption, and to actually meet these optimal performances, the PMSM torque has to accurately match this optimal demand. Accuracy and repeatability are key points relating to the torque control of PMSM in automotive applications.

Regarding industrial constraints, assuming torque or flux sensors available to meet the previously mentioned requirements is not reasonable. This point makes lean towards a model-based approach where the main challenges are the determination of the rotor position and the estimation of the physical parameters involved in torque production, such as the saliency parameters or the permanent magnet flux.

The torque produced by a PMSM primarily relies on the interaction of the magnetic field due to stator currents with the rotor magnets. Precise torque production is achieved when the angular position of the rotor is known, in order to phase both interacting magnetic fields. Several papers have addressed the determination of the rotor position from current measurements, usually referred to as sensorless control. Existing techniques rely on the determination of an electrical phenomenon related to the rotor position. This may either be some back-electromotive force observation while the motor is in operation, or saliency parameters determination at standstill, see [7], [8] for an excellent overview. Moreover, as the motor temperature rises along the driving cycle, the magnetic field due to the magnets decreases. Therefore, it is obvious that a drift in the produced torque may occur if the control is not adapted with this material change [19]. Manufacturers privileged high saliency ratio, to end up with lighter machines especially suited for vehicle applications [9]. Saliency is also responsible for an extra component of the torque that may not be neglected. This point is also material for the proposed objectives [2]. Estimating the temperature dependant parameters and the saliency parameters has been also addressed in many control and electric machines papers [4], [6], [11].

This paper presents an adaptive torque control scheme for PMSM in automotive applications. All the relevant physical parameters involved in the torque production are estimated online, so that prerequisite information about the motor are drastically limited[1]. A preliminary estimation phase, maintaining the motor at zero velocity, allows to accurately determine the initial rotor angular position, as well as saliency and the armature resistance. High-frequency alternating voltages are injected to the motor windings, and current measurements are then used to obtain the previously mentioned parameters via the minimization of a quadratic index. No specific hardware is required, and computation

[1]Only the number of poles pairs and a rough estimate of the magnetic flux are required.

978-1-4244-8218-4/10/$26.00 ©2010 IEEE

efforts are within admissible reach. To maintain a precise control of the torque while in operation, and in spite of thermal effects along the driving cycle, a nonlinear observer is designed to estimate online both the windings resistance and the magnetic flux [6], [10]. This observer is based on the work developed in [1]. It essentially relies on the invariant manifold based approach which allows to shape the dynamics of the estimation error. In this application, the observer developed is based on speed and current measurements, as well as the rotor position and the saliency parameters previously determined. These physical parameters are then fed to an online optimization algorithm in charge of adapting the reference dq-axis currents to maintain the desired torque. This indirect adaptive scheme minimizes the copper losses, from below the base speed, deep into the flux weakening area.

The structure of the paper is as follows. The mathematical model used throughout this work, as well as the different assumptions and considered experimental conditions, are first presented in Section II. The initial identification phase performed at standstill is then presented in Section IV. The online observer for thermal drift estimation, together with its convergence proof, are then given in Section V. Some details are then given on the overall control scheme in Section VI, more specifically focusing on the online optimization previously mentioned. Some simulation and experimental results are given in Section VII to assess the relevancy of our approach. We wrap up the paper with some concluding remarks.

II. Permanent Magnet Synchronous Motors Modeling

The classical modeling [5], [14] used throughout this paper is given by the following set of equations expressed in the dq-frame:

$$\begin{aligned} L_d \frac{di_d}{dt} &= -Ri_d + p\omega L_q i_q + v_d \\ L_q \frac{di_q}{dt} &= -Ri_q - p\omega \left(L_d i_d + \sqrt{\frac{3}{2}}\Phi \right) + v_q \\ \tau &= p\sqrt{\frac{3}{2}}\Phi i_q + p\left(L_d - L_q\right) i_d i_q \end{aligned} \tag{1}$$

where (i_d, i_q) and (v_d, v_q) are respectively the currents and input voltages in the dq-axis frame, ω is the rotary speed of the rotor shaft and τ is the torque provided by the motor. The different parameters appearing in (1) are the stator windings resistance R, the flux due to the rotor magnets Φ, the inductances (L_d, L_q) modeling saliency and finally p the number of poles pairs. Except for the latter, we shall assume that these parameters are unknown, and that Φ and R are temperature dependent, while L_d and L_q are constant.

In the following, we shall also make use of the equations (1) expressed in the abc-axis frame, both sets of equations being linked through the Park transform. Actually, current measurements and voltage inputs are only available in this frame, namely the currents (i_a, i_b, i_c) are measured, and the three-phase voltages (v_a, v_b, v_c) are controlled. The information about the absolute rotor position θ is missing, only the rotary velocity $\omega = \dfrac{d\theta}{dt}$ and the relative displacements around the initial angle are known.

III. Control Problem

A. Problem formulation

Given this context, from now on, our goal is to design a field-oriented control scheme for the torque τ to track a time-varying torque demand $\tau^\star$.

B. Proposed solution strategy

The solution to the problem stated in Section III-A proceeds along the following steps:

1) Estimate the initial angular position of the rotor. A technique maintaining the motor at rest, and relying on current measurements, is detailed in the sequel of the paper. By doing so, we also get an estimation for the inductances values (L_d, L_q), as well as the resistance R.
2) Once θ is known, (i_d, i_q) are assumed measured, and (v_d, v_q) controlled.
3) To perform an accurate control of τ, determining Φ and R in operation is a task of prime interest since these parameters are known to vary as the motor temperature changes. We propose an observer, relying only on velocity and current measurements, featuring global convergence towards the actual values of R and Φ.
4) Finally, we eventually use the parameters estimated online and at standstill to compute in real time the references $\left(i_d^\star, i_q^\star\right)$ making the electromagnetic torque follow the reference signal $\tau^\star$, and minimizing the copper losses.

IV. Initialization Parameters Identification

A. Principle

We design a technique injecting high-frequency currents within the stator windings, so that a high-frequency torque is created. For automotive applications, the mechanical systems connected to the motor obviously feature dry friction and a low-pass filtering behavior. For these reasons, the proposed solution is claimed to maintain the motor shaft at rest. The inverter is driven in a non conventional way, to actually end up with alternating polarity phase-to-phase voltages. Typical implementation consists in connecting the phase a to the dc link, while both phases b and c are connected up together, and then switch to the converse setup. The same is then performed to apply an alternating voltage between the phase b (resp. c) and the phases a and c (resp. b and a) connected up together.

B. Estimation algorithm

The available measurements recorded during this experimental protocol may be related to the parameters to estimate. They are obtained by minimizing a quadratic index, as exposed in the following proposition.

Proposition 1: An estimated value of the initial rotor position is given by:

$$\begin{aligned} \widehat{\theta} &= \arg\min_{\theta\in[0,\frac{\pi}{p}[} \left(\sum_i \int_0^{t_i} \big(y_i(t) - \Phi_i(t,\theta)\lambda(\theta)\big)^2 dt \right) \\ s.t. \quad & (i) \quad \lambda_1(\theta) \leq \lambda_2(\theta) \end{aligned} \tag{2}$$

where $\lambda(\theta) = (\lambda_1(\theta) \quad \lambda_2(\theta) \quad \lambda_3(\theta))^\top$ is a mapping defined by (11), and Φ_i and y_i are defined by (8). Estimated values of the parameters R, L_d and L_q are given by

$$\left(\widehat{L}_d \, \widehat{L}_q \, \widehat{R}_0\right)^\top = \lambda\left(\widehat{\theta}\right). \tag{3}$$

Proof: In the following proof, thanks to equation (6), we first relate the four unknown parameters to the available measurements, namely the line currents and phase-to-phase voltages. We then form a one-dimensional optimization index in equation (10). In the abc-axis frame, when the motor is at rest, the line voltage V_a is given by:

$$\begin{aligned} V_a &= Ri_a + \frac{d\varphi_a}{dt} \\ &= Ri_a + \sqrt{\frac{2}{3}}\frac{d}{dt}\left(L_d i_d \cos(p\theta) + L_q i_q \sin(p\theta)\right) \end{aligned} \tag{4}$$

where the first line of (4) is obtained by applying the ohmic and Faraday's laws with the flux φ_a, and the second line is derived by expressing φ_a in the dq-axis frame according to the inverse Park transform and the equation (1) with $\omega = 0$. Applying the Park transform together with the relation $i_a + i_b + i_c = 0$, the equation (4) may be rewritten to only rely on i_a and i_b as:

$$V_a = \left(\frac{dI_{ab}}{dt} M_a(\theta) \quad i_a\right)\mu, \tag{5}$$

where $\mu^\top = (L_d \quad L_q \quad R)$, M_a is a mapping from $\mathbb{R}$ to $\mathbb{R}^{2\times 2}$ and $I_{ab} = (i_a \quad i_b)$. Equations similar to (5) may be derived for the voltages V_b and V_c. The phase-to-phase voltages, assumed to be known, are eventually given by:

$$\begin{aligned} V_a - V_b &= \left(\frac{dI_{ab}}{dt} M\left(\theta\right) \quad \gamma^\top I_{ab}\right)\mu \\ V_b - V_c &= \left(\frac{dI_{bc}}{dt} M\left(\theta - \frac{2\pi}{3}\right) \quad \gamma^\top I_{bc}\right)\mu \\ V_c - V_a &= \left(\frac{dI_{ca}}{dt} M\left(\theta + \frac{2\pi}{3}\right) \quad \gamma^\top I_{ca}\right)\mu \end{aligned} \tag{6}$$

where $\gamma^\top = (1 \ -1)$, I_{bc} and I_{ca} are defined similarly to I_{ab} and M is a mapping from $[0, \frac{\pi}{p}[$ to $\mathbb{R}^{2\times 2}$ defined as follows:

$$M(\theta) = \begin{pmatrix} 2\cos\left(p\theta\right)^2 - \frac{1}{2} & -\cos\left(p\theta\right)^2 + \frac{3}{2} \\ 2\sin\left(p\theta\right)\sin\left(p\theta + \frac{2\pi}{3}\right) & 2\cos\left(p\theta\right)\cos\left(p\theta + \frac{2\pi}{3}\right) \end{pmatrix} \tag{7}$$

For the estimation purpose, rather than this differential formulation, we shall use an integral form of the set of equations (6). Let's introduce some further notations with:

$$\begin{aligned} y_a(t) &= \int_0^t \left(V_a(t') - V_b(t')\right) dt' \\ \Phi_a(t,\theta) &= \begin{pmatrix} \big(I_{ab}(t) - I_{ab}(0)\big) M(\theta) \\ \int_0^t \gamma^\top I_{ab}(t') dt' \end{pmatrix} \end{aligned} \tag{8}$$

The real-valued function y_b (resp. y_c) and the mapping Φ_b (resp. Φ_c) may be defined in the same way as (8). We end up with the following set of equations, that we shall use to estimate the unknown parameters:

$$y_a = \Phi_a(t,\theta)\mu, \quad y_b = \Phi_b(t,\theta)\mu, \quad y_c = \Phi_c(t,\theta)\mu \tag{9}$$

The following index, $\frac{\pi}{p}$-periodic in θ, may be formed:

$$\mathcal{J}(\theta,\mu) = \sum_{i\in\{a,b,c\}} \int_0^{t_i} \left(y_i(t) - \Phi_i(t,\theta)\mu\right)^2 dt, \tag{10}$$

where the summation extends over all the available experiments of time length t_i. Practically speaking, t_a (resp. t_b and t_c) is the time during which alternating-polarity voltages are applied between the phases a and b (resp. b and c, c and a), y_a and Φ_a (resp. y_b and Φ_b, y_c and Φ_c) are formed with data collected during this experiment.

For any given θ, minimizing $\mathcal{J}(\theta,\mu)$ with respect to μ has an analytical solution, parameterized by θ. We denote it $\lambda\left(\theta\right)$, and it is given by:

$$\lambda(\theta) = \left(\sum_i \int_0^{t_i} \Phi_i^\top \Phi_i dt\right)^{-1} \left(\sum_i \int_0^{t_i} \Phi_i^\top y_i dt\right). \tag{11}$$

Minimizing $\mathcal{J}(\theta,\mu)$ with respect to both θ and μ actually comes down to the one-dimensional problem of equation (2), where $\lambda(\theta)$ is defined by (11). The index of equation (2) is $\frac{\pi}{2p}$-periodic, and the ambiguity over $[0, \frac{\pi}{p}[$ is dispelled by recalling that $L_d < L_q$, which reads that $\lambda_1\left(\widehat{\theta}\right)$ has to be smaller than $\lambda_2\left(\widehat{\theta}\right)$. For that particular $\widehat{\theta}$, we then get the estimate $\widehat{\eta}$ with $\lambda\left(\widehat{\theta}\right)$, which is neither more nor less than equation (3). ■

Additional information is needed to solve the problem over $[0, \frac{2\pi}{p}[$. This may be achieved by either looking at magnetic saturation curves, or by detecting the velocity sign as soon as the rotor starts rotating. For obvious reasons, the initial mechanical position of the rotor may not be determined over $[0, 2\pi[$, given the $\frac{2\pi}{p}$-periodic layout of the magnetic poles.

V. Online PMSM Parameters Observation

Following the observer methodology defined in [10], in this section, we construct an estimator for the PMSM parameters remaining so far unknown and subject to temperature related variations. The estimator assumes that these

parameters change very slowly with the time, which boils down to assuming that the motor temperature exhibits a slow evolution along the driving cycle. This assumption has great significance, since it provides an equation for the observer design and enables one to estimate these parameters. The main result is given by the following proposition.

Proposition 2: For some positive scalars α_1 and α_2, and $\left(\widehat{L}_d, \widehat{L}_q\right)$ given by proposition 1, the following reduced order observer:

$$\begin{aligned}
\dot{\xi}_1 &= \frac{\alpha_1}{L_d} i_d \left(-\widehat{R} i_d + p\omega L_q i_q + v_d\right) \\
\dot{\xi}_2 &= \frac{\alpha_2}{L_q} \left(-\widehat{R} i_q - p\omega L_d i_d - \sqrt{\frac{3}{2}}\widehat{\Phi} p\omega + v_q\right) \\
\widehat{R} &= -\frac{\alpha_1}{2} i_d^2 + \xi_1 \\
\widehat{\Phi} &= -\alpha_2 i_q + \xi_2
\end{aligned} \tag{12}$$

guarantees global asymptotic convergence of $\widehat{R}$ and $\widehat{\Phi}$ towards the respective actual values of R and Φ despite thermal drift.

Proof: The ongoing proof follows the lines of the approach proposed in [10]. Let's first define

$$\eta = \begin{bmatrix} R & \phi \end{bmatrix}^\top, \tag{13}$$

and the parameters observer structure is given by:

$$\widehat{\eta} = \xi + \beta\left(i_d, i_q\right), \tag{14}$$

where $\xi \in \mathbb{R}^2$ is the observer state and

$$\beta(i_d, i_q) = \begin{bmatrix} \beta_1(i_d, i_q) & \beta_2(i_d, i_q) \end{bmatrix}^\top \tag{15}$$

is a mapping to be defined. Denote z the error variable

$$z = \hat{\eta} - \eta = \xi + \beta(i_d, i_q) - \eta, \tag{16}$$

which dynamics is given by

$$\begin{aligned}
\dot{z} &= \dot{\xi} + \tfrac{\partial \beta}{\partial i_d}\tfrac{1}{L_d}\left(-\left(\xi_1 + \beta_1 - z_1\right) i_d + p\omega L_q i_q + v_d\right) \\
&+ \tfrac{\partial \beta}{\partial i_q}\tfrac{1}{L_q}\left(-\left(\xi_1 + \beta_1 - z_1\right) i_q - p\omega L_d i_d\right) \\
&+ \tfrac{\partial \beta}{\partial i_q}\tfrac{1}{L_q}\left(-\sqrt{\tfrac{3}{2}} p\omega\left(\xi_2 + \beta_2 - z_2\right) + v_q\right).
\end{aligned} \tag{17}$$

Therefore the observer dynamics $\dot{\xi}$ can be selected for the error variable to be autonomous, namely:

$$\begin{aligned}
\dot{\xi} &= -\frac{\partial \beta}{\partial i_d}\frac{1}{L_d}\left(-\left(\xi_1 + \beta_1\right) i_d + \omega L_q i_q + v_d\right) - \frac{\partial \beta}{\partial i_q}\frac{1}{L_q} v_q \\
&- \frac{\partial \beta}{\partial i_q}\frac{1}{L_q}\left(-\left(\xi_1 + \beta_1\right) i_q - \omega L_d i_d - \sqrt{\frac{3}{2}}\omega\left(\xi_2 + \beta_2\right)\right),
\end{aligned}$$

so that the error dynamics reads:

$$\dot{z} = \begin{pmatrix} \frac{\partial \beta_1}{\partial i_d} & \frac{\partial \beta_1}{\partial i_q} \\ \frac{\partial \beta_2}{\partial i_d} & \frac{\partial \beta_2}{\partial i_q} \end{pmatrix} \begin{pmatrix} \frac{i_d}{L_d} & 0 \\ \frac{i_q}{L_q} & \frac{\sqrt{\frac{3}{2}}\omega}{L_q} \end{pmatrix} z. \tag{18}$$

Selecting the functions

$$\beta_1(i_d) = -\frac{\alpha_1}{2} i_d^2, \quad \beta_2(i_q) = -\alpha_2 i_q \tag{19}$$

with $\alpha_1, \alpha_2 > 0$ ensures that the equilibrium $z = 0$ is globally asymptotically stable. Moreover, using the candidate Lyapunov function $V(z) = \frac{1}{2} z^\top P z$ with

$$P = \begin{bmatrix} P_1 & -\frac{\alpha_2}{L_q} i_q \\ -\frac{\alpha_2}{L_q} i_q & \frac{\alpha_1}{L_d} i_d^2 + \frac{\alpha_2}{L_q}\sqrt{\frac{3}{2}}\omega \end{bmatrix}, \tag{20}$$

and $P_1 > \frac{\alpha_2^2 L_d i_q^2}{\alpha_1 L_q^2 i_d^2}$, it can be shown that

$$\lim_{t \to \infty} \left(\eta - \widehat{\eta}\right) = 0 \tag{21}$$

provided that i_d, ω are bounded away from zero. As a result, from (13)-(16) an asymptotic estimate of R and ϕ is given by $\xi_1 + \beta_1$ and $\xi_2 + \beta_2$ respectively. ■

VI. Controller Design

Through the propositions 1 and 2, all the relevant parameters for the accurate torque control are determined online, either at standstill or in operation as some of them may undergo variations. We shall make use of this information to track the time-varying reference $\tau^\star$, despite the temperature dynamics. The following two-step approach is considered:

- time-varying references $i_d^\star$ and $i_q^\star$ are computed online to respond to the torque request $\tau^\star$ and minimize the copper losses,
- local PI controllers are implemented for i_d and i_q to respectively rally the references $i_d^\star$ and $i_q^\star$.

The latter point is rather classical, while the first requires further information. It significantly differs from usual approaches (see [4] for instance) relying on look-up tables, computed offline with the nominal values of physical parameters. When operating above the base speed, classical techniques are supplemented with a closed loop control to get rid of parameters uncertainties. We suggest the unified method of the proposition 3 that allows to minimize copper losses from below base speed to the field weakening area, while being robust to parameters variations.

Proposition 3: The torque adaptation scheme is performed by the following optimization problem

$$\begin{aligned}
\left(i_d^\star, i_q^\star\right) &= \arg \min_{(i_d, i_q) \in \mathbb{R}^2} \left(i_d^2 + i_q^2\right) \\
\text{s.t.:} \quad \text{(i)} &\quad \tau^\star = p\sqrt{\frac{3}{2}}\widehat{\Phi} i_q + p\left(\widehat{L}_d - \widehat{L}_q\right) i_d i_q \\
\text{(ii)} &\quad i_d^2 + i_q^2 \leq i_{\max}^2 \\
\text{(iii)} &\quad v_d^2 + v_q^2 \leq v_{\max}^2
\end{aligned} \tag{22}$$

to solve online, where (iii) is given by the equations (1) in steady state, $\widehat{L}_d$ and $\widehat{L}_q$ by the proposition 1 and $\widehat{R}$ and $\widehat{\Phi}$ by the proposition 2.

Fig. 1. Experimental setup.

VII. Results

A. Experimental Setup

The performances of the previously designed adaptive torque controller are experimentally validated on a testbed made up of two PMSM, connected through a shaft featuring a torque sensor delivering accurate torque measurements. This setup is illustrated on figure 1. These two drives have respective rated power of 1.7kW and 2.2kW, and and similar rated speed of 6000rpm. They are respectively intended to deliver a desired torque for the first one, and control the rotary speed of the shaft for the latter. The torque control strategies previously discussed are implemnted in a voltage inverter connected to the first machine, and the actually provided torque to the shaft may be monitored thanks to the torque sensor.

Preliminary experiments, requiring dedicated pieces of hardware, are conducted to determine:

- the actual position θ of the shaft, by making use of back-emf measurements together with information given by the incremental angular sensor,
- the actual value of the magnetuc flux $\Phi = 0.075$Wb, for ambient temperature conditions, thanks to back-emf measurements,
- the actual value of the stator resistance $R = 0.25\Omega$, for ambient temperature conditions, by applying a constant voltage to the windings and monitoring the resulting current.

Concerning the inductances (L_d, L_q), the technical datasheet of the drive gives a rough estimate of $L_d = L_q = 0.77mH$, without distinguishing between the direct and quadrature inductances. All these parameters values are the reference values that our different estimation techniques have to converge to, though some a priori doubts may be expressed about the reference values of the inductances.

B. Initial Identification

The experimental results of the identification technique given in proposition 1 are showed in figure 2. The position of the shaft is manually varied, and the identification algorithm is executed for each position, without any knownledge of the actual position. We show the estimated values of $p\widehat{\theta}$ on figure 2(a), $\widehat{R}_0$ on figure 2(b) and finally the inductances $\left(\widehat{L}_d, \widehat{L}_q\right)$ on figure 2(c). These plots clearly assess the accuracy of the method in determining the initial position, as well as the inductances despite unknown armature resistance. This point is consistant with the use of these estimated values for precise torque control, as the main concern of this paper.

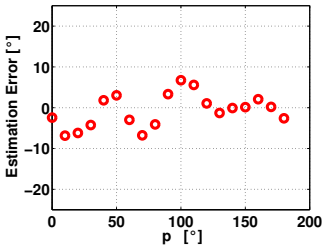

(a) Angle estimation error.

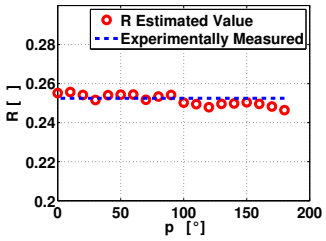

(b) Resistance estimation.

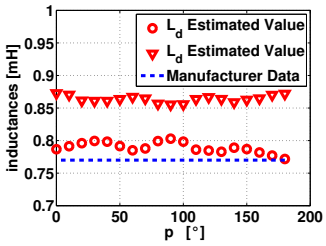

(c) Inductances estimation.

Fig. 2. Experimental results of the identification at standstill.

C. In Operation Estimation

The experimental results of the estimation of the flux and the resistance as the motor is rotating are respectively given on the figures 3(a) and 3(b). The convergence of $\widehat{\Phi}$ towards the actual value of Φ begins as soon as the shaft starts rotating, around $t = 8s$. The convergence of $\widehat{R}$ towards the reference R occurs as soon as a non-zero i_d^* is given to the controller, which happens around $t = 34s$. The effectiveness of the observer is thus experimentally validated for the nominal values of these parameters.

D. Adaptive Torque Control

We now provide simulation results of the whole adaptive scheme. These results are obtained thanks to a complete

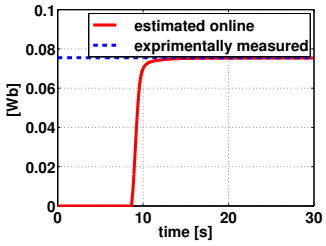

(a) Online estimation of the flux.

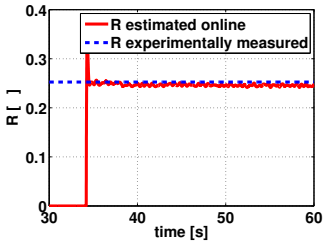

(b) Online estimation of the resistance.

Fig. 3. Experimental results of the online parameters observation.

modeling in the MATLAB/SIMULINK environment of the experimental testbench (see figure 1), including the dependency of Φ and R on temperature through a power balance featuring ohmic losses. For the nominal operating conditions $\tau^* = 2.8$Nm and $\omega = 6000$rpm, our goal is to compare the adaptive scheme to a classical torque controller based on the knowledge of Φ and R for the ambient temperature conditions. These results are given on figure 4.

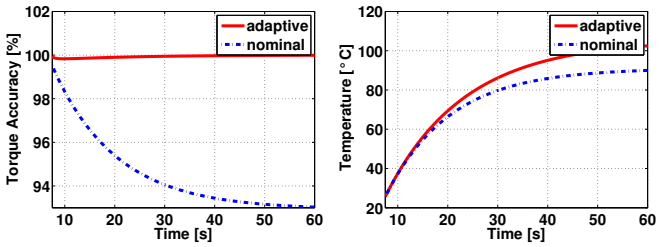

(a) Torque accuracy τ/τ^*.

(b) Temperature.

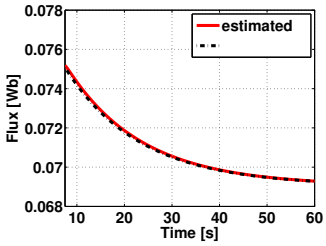

(c) Magnetix fluxe Φ and $\widehat{\Phi}$.

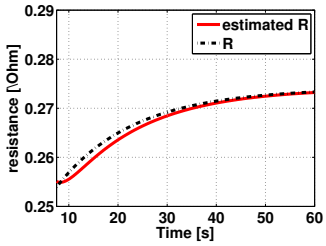

(d) Resistance R and $\widehat{R}$.

Fig. 4. Simulation results in nominal operating conditions. Comparison of the adaptive scheme to a classical controller.

By first having a look at the figures 4(d) and 4(c), it can be noted that the observer given by the proposition 2 enables to precisely estimate online Φ and R while they are subject to significant deviations due to the temperature rise of the motor (see figure 4(b). These estimated values are then fed to an online routine computing the operating point so as to both guarantee the torque accuracy despite the thermal drift, and minimize the copper losses within the windings. As illustrated by the figure 4(a), once the estimated magnetic flux has reached the actual value Φ, the actual torque converges towards the desired value. On top of that, note that by injecting higher current levels to satisfy the torque demand, the temprature rise is clearly amplified under operation with the adaptive scheme.

VIII. Conclusion

The theoretical background exposed in the propositions 1, 2 and 3 enabled to design an adaptive torque control, especially suited for vehicle applications. Preliminary experimental results showed the relevancy of the approach, especially by providing satisfactory results for the estimation of the inductances at standstill, and the temperature dependent parameters while the motor is rotating. Additionnal simulation results illustrated the ability of the proposed technique to maintain the actual torque to its desired value, even if the motor is subject to an unknown or unmeasured temperature rise. Future work will consist in using these online estimation of R and Φ together with a thermal modeling of the motor to design an online sensorless thermal monitoring of PMSM used in automative applications.

References

[1] A. Astolfi, D. Karagiannis, and R. Ortega. *Nonlinear and Adaptive Control with Applications*. Springer–Verlag, London, 2008.

[2] D. Basic, F. Malrait, and P. Rouchon. Modeling magnetic saturation and saliency effects via euler lagrange models with complex currents for three phase permanent magnet machines. *Ifac Workshop on Engine and Powertrain Control, Simulation and Modelling*, December 2009.

[3] A. Chasse, G. Hafidi, P. Pognant Gros, and A. Sciarretta. Supervisory control of hybrid powertrains: an experimental benchmark of offline optimization and online energy management". *IFAC Workshop on Engine and Powertrain Control, Simulation and Modeling, France*, December 2009.

[4] X. Chen, R. Thornton, M. Edington, and R. Lewis. Accurate torque control of ipm machines for isg hybrid vehicle applications. *14th Asia Pacific Automotive Engineering Conference Hollywood, USA*, August 2007.

[5] J. N. Chiasson. *Modeling and High Performance Control of Electric Machines*. IEEE Press, 2005.

[6] Q. Han, C. Ham, and R. Phillips. Pmsm nonlinear robust control for temperature compensation. *Proceedings of the Thirty-Sixth Southeastern Symposium on System Theory*, pages 88 – 91, 2004.

[7] J. Holtz. Sensorless control of induction motor drives. *Proceedings of the IEEE*, 90, No 8:1359 – 1394, August 2002.

[8] S. Ichikawa, M. Tomita, S. Doki, and S Okuma. Sensorless control of permanent magnet synchronous motors using online parameter identification based on system identification theory. *IEEE Transactions on Industrial Electronics*, 53, No 2:363 – 372, April 2006.

[9] M. Kamiya. Development of traction drive motors for the toyota hybrid system. *2005 International Power Electronics Conference*, pages 1474 – 1481, 2005.

[10] D. Karagiannis and A. Astolfi. Observer design for a class of nonlinear systems using dynamic scaling with application to adaptive control. *47 th IEEE Conference on Decision and Control, Cancun, Mexico*, pages 2314–2319, December 2008.

[11] G. Kenne, T. Ahmed-Ali, F. Lamnabhi-Lagarrigue, and A. Arzande. Time varying parameter identification of a class of nonlinear systems with application to online rotor resistance estimation of induction motors. *2006 IEEE International Symposium on Industrial Electronics*, 1:301 – 306, July 2006.

[12] P. Kundur. *Power System Stability and Control*. McGraw–Hill, 1994.

[13] K. I. Laskaris and A. G. Kladas. Internal permanent magnet motor design for electric vehicle drive. *IEEE Transactions on Industrial Electronics*, 57, No 1:138 – 145, January 2010.

[14] W. Leonhard. *Control of Electrical Drives*. Springer, 3rd edition, 2001.

[15] R. Monajemy and R. Krishnan. Control and dynamics of constant power loss based operation of permanent magnet synchronous motor drive system. *IEEE Transactions on Industrial Electronics*, 48, No 4:839 – 844, August 2001.

[16] V. Petrovic, R. Ortega, and A. M. Stankovic. Interconnection and damping assignment approach to control of pm synchronous motors. *IEEE Transactions on Control Systems Technology*, 9, No 6:811 – 820, November 2001.

[17] P. Pillay and R. Krishnan. Modeling of permanent magnet motor drives. *IEEE Transactions on Industrial Electronics*, 35, No 4:537 – 541, November 1988.

[18] A. Sciarretta, M. Back, and L. Guzzella. Optimal control of parallel hybrid electric vehicles. *IEEE Transactions on Control Systems Technology*, 12, No 3:352 – 363, Mai 2004.

[19] T. Sebastian. Temperature effects on torque production and efficiency of pm motors using ndfeb magnets. *IEEE Transactions on Industry Applications*, 31, No 2:353 – 357, April 1995.